Ferron *et al. Molecular Brain* (2022) 15:43
https://doi.org/10.1186/s13041-022-00930-x

Molecular Brain

SHORT REPORT

Open Access

$Ca_V\beta$-subunit dependence of forward and reverse trafficking of $Ca_V1.2$ calcium channels

Laurent Ferron, Sydney D. Guderyan†, Ethan J. Smith† and Gerald W. Zamponi*

Abstract

Auxiliary $Ca_V\beta$ subunits interact with the pore forming $Ca_V\alpha_1$ subunit to promote the plasma membrane expression of high voltage-activated calcium channels and to modulate the biophysical properties of Ca^{2+} currents. However, the effect of $Ca_V\beta$ subunits on channel trafficking to and from the plasma membrane is still controversial. Here, we have investigated the impact of $Ca_V\beta1b$ and $Ca_V\beta2a$ subunits on plasma membrane trafficking of $Ca_V1.2$ using a live-labeling strategy. We show that the $Ca_V\beta1b$ subunit is more potent in increasing $Ca_V1.2$ expression at the plasma membrane than the $Ca_V\beta2a$ subunit and that this effect is not related to modification of intracellular trafficking of the channel (i.e. neither forward trafficking, nor recycling, nor endocytosis). We conclude that the differential effect of $Ca_V\beta$ subunit subtypes on $Ca_V1.2$ surface expression is likely due to their differential ability to protect $Ca_V1.2$ from degradation.

Keywords: Calcium channel, Trafficking, $Ca_V\beta$ auxiliary subunits

Introduction

Calcium influx generated by voltage-gated calcium channels plays a critical role in neuronal functions such as excitability and gene transcription [1, 2]. High-voltage-activated (HVA) Ca^{2+} channels are formed by assembly of several subunits including the pore forming $Ca_V\alpha_1$ subunit and auxiliary $Ca_V\alpha_2\delta$ and $Ca_V\beta$ subunits [3].

Among HVA channels, $Ca_V1.2$ is the most abundant in the mammalian brain [4] and it is localized in clusters in dendritic shafts and spines [5, 6]. Auxiliary $Ca_V\beta$ subunits are key modulators of channel biophysical properties and their targeting to the plasma membrane [7, 8]. Four $Ca_V\beta$ isoforms have been identified and they are all expressed in the brain. They contain 2 highly conserved domains: a Src Homology 3 domain and a guanylate kinase domain and variable N-terminal, Hook and C-terminal domains. The guanylate kinase domain binds to the α-interacting domain (AID) in the intracellular I–II loop of $Ca_V\alpha_1$ subunits. The binding of $Ca_V\beta$ to the AID protects $Ca_V\alpha_1$ from degradation by the proteasome [9]. However, the impact of $Ca_V\beta$ subunits on the trafficking of $Ca_V1.2$ to and from the plasma membrane is still a matter of debate [10–12].

In this study, we investigated the effects of two $Ca_V\beta$ subunits, the cytoplasmic $Ca_V\beta1b$ subunit and the membrane anchored (palmitoylated) $Ca_V\beta2a$ subunit [13, 14], on plasma membrane trafficking of $Ca_V1.2$ using a live-labeling strategy based on a $Ca_V1.2$ construct tagged with bungarotoxin binding sites. We show that $Ca_V\beta1b$ is more potent in increasing $Ca_V1.2$ expression at the plasma membrane than $Ca_V\beta2a$ and that this effect is not linked to modification of either forward trafficking, recycling or endocytosis. We suggest that the effect of different $Ca_V\beta$ subunits on $Ca_V1.2$ surface expression is likely

†Sydney D. Guderyan and Ethan J. Smith contributed equally to this work

*Correspondence: zamponi@ucalgary.ca

Department of Physiology and Pharmacology, Alberta Children's Hospital Research Institute, Hotchkiss Brain Institute, Cumming School of Medicine, University of Calgary, Calgary, AB, Canada

due to their differential ability to protect $Ca_V1.2$ from degradation.

Materials and methods

Molecular biology

Alpha-bungarotoxin binding sites (BBS: WRYYESSLEPYPD) were inserted between the S5 and the P loop of domain II of $Ca_V1.2$ (downstream Q683: FDEMQ-BBS-TRRST) using standard molecular biology techniques. Briefly, two oligonucleotides coding for a BBS and flanked by *Mlu*I restriction sites (oligo A: 5′-ACGCGTCGGACCGGTTGGAGATACTACGAGAGCTCCCTGGAGCCCTACCCTGACCGT A-3′; oligo B: 5′-CGCGTACGGTCAGGGTAGGGCTCCAGGGAGCTCTCGTAGTATCTCCAACCGGTCCGA-3′) were synthesized, annealed and cloned into pMT2 $Ca_V1.2$ construct (rat brain $Ca_V1.2$ from T. Snutch; GenBank: M67515.1) linearized with *Mlu*I. Correct orientation and location of oligonucleotide cloning were confirmed by sequencing the plasmids. A triple BBS construct was generated.

Cell culture and transfection

tsA-201 cells were cultured as previously described [15]. Cells were transfected with plasmid encoding rat $Ca_V1.2$ (WT or BBS), rat $Ca_V\alpha_2\delta$-1 (GenBank: NM_012919.3) and either rat $Ca_V\beta$1b (GenBank: NM_017346.1) or rat $Ca_V\beta$2a (GenBank: NM_053851.1) using the calcium phosphate method. For electrophysiological experiments, cDNA encoding GFP was co-transfected and used as a transfection marker. Apart from dynamin1 K44E [16] which was cloned into pcDNA3.1, all constructs were cloned into the pMT2 vector.

Electrophysiology recordings

Twenty-four hours after transfection, tsA-201 cells were transferred to a 30 °C incubator for 48 h before being used for experiments. Whole-cell patch-clamp recordings were performed and analyzed as described previously [15]. Briefly, currents were recorded at room temperature (22–24 °C) using an Axopatch 200B amplifier and pClamp 9.2 software. Patch pipettes were filled with a solution containing the following (in mM): 130 CsCl, 2.5 $MgCl_2$, 10 HEPES, 5 EGTA, 3 Na-ATP, 0.5 Mg-GTP, pH 7.4. The external solution contained the following (in mM): 132.5 CsCl, 1 $MgCl_2$, 10 HEPES, 5 $BaCl_2$, 10 glucose, pH 7.4. Current–voltage relationships were obtained by applying 250 ms pulses ranged from −50 to +50 mV in 5 mV increment from a holding potential of −100 mV. Current density–voltage relationships were fitted with a modified Boltzmann equation as follows: $I = (G_{max} \times (V - V_{rev}))/(1 + \exp(-(V - V_{50,act})/k))$, where I is the current density (in pA/pF), G_{max} is the maximum conductance (in nS/pF), V_{rev} is the reversal potential, $V_{50,act}$ is the midpoint voltage for current activation and k is the slope factor.

Trafficking assays and confocal microscopy

tsA-201 cells were plated onto glass-bottomed dishes (MatTek Corp., Ashland, MA) precoated with poly-L-lysine and transfected as described above. After 3 days expression, cells were washed twice with Krebs–Ringer solution with HEPES (KRH) (in mM; 125 NaCl, 5 KCl, 1.1 $MgCl_2$, 1.2 KH_2PO_4, 2 $CaCl_2$, 6 Glucose, 25 HEPES, 1 $NaHCO_3$). For endocytosis experiments, cells were incubated with 10 µg/ml α-bungarotoxin Alexa Fluor® 488 conjugate (BTX488) (Thermo Fisher Scientific) at 17 °C for 30 min. The unbound BTX488 was removed by washing with KRH, and the labelled cells were returned to 37 °C. Endocytosis was terminated by fixing the cells with cold 4% PFA in PBS for 5 min, and then permeabilized with 0.05% Triton X-100 in PBS for 10 min. Cells were blocked with 10% FBS in PBS for at least 30 min and incubated with the primary Ab (rabbit anti-$Ca_V1.2$, 1:200, Alomone labs) for 1 h at room temperature. Samples were washed and incubated with secondary conjugated Ab anti-rabbit AF594 (1:500; Thermo Fisher Scientific) for 1 h at room temperature. After washing, samples were covered with SlowFadeTM Gold antifade mountant (Thermo Fisher Scientific). For the forward trafficking assay, the cells were incubated with 10 µg/ml unlabeled α-bungarotoxin (BTX; Thermo Fisher Scientific) at 17 °C for 30 min. The unbound BTX was washed off with KRH, and the cells were then incubated with 10 µg/ml BTX488 in KRH at 37 °C. To stop the reaction, cells were washed twice with cold KRH and then fixed with 4% PFA in PBS. Brefeldin A (BFA; 200 ng/ml (0.71 µM); Sigma-Aldrich) in 0.4% DMSO was added to the cells in FBS-free culture medium for 4 h before the experiment, and during the experiment in KRH buffer. Cells were examined on a Leica SP8 confocal microscope using a 63×/1.4 numerical aperture oil-immersion objective in 16-bit mode. Acquisition settings, chosen to ensure that images were not saturated, were kept constant for each experiment.

Statistical analysis

Data are given as mean ± SEM. Statistical comparisons were performed using paired and unpaired Student's t tests, as appropriate, using SigmaPlot 14.5 or Prism GraphPad. Differences were considered to reach statistical significance when $p < 0.05$.

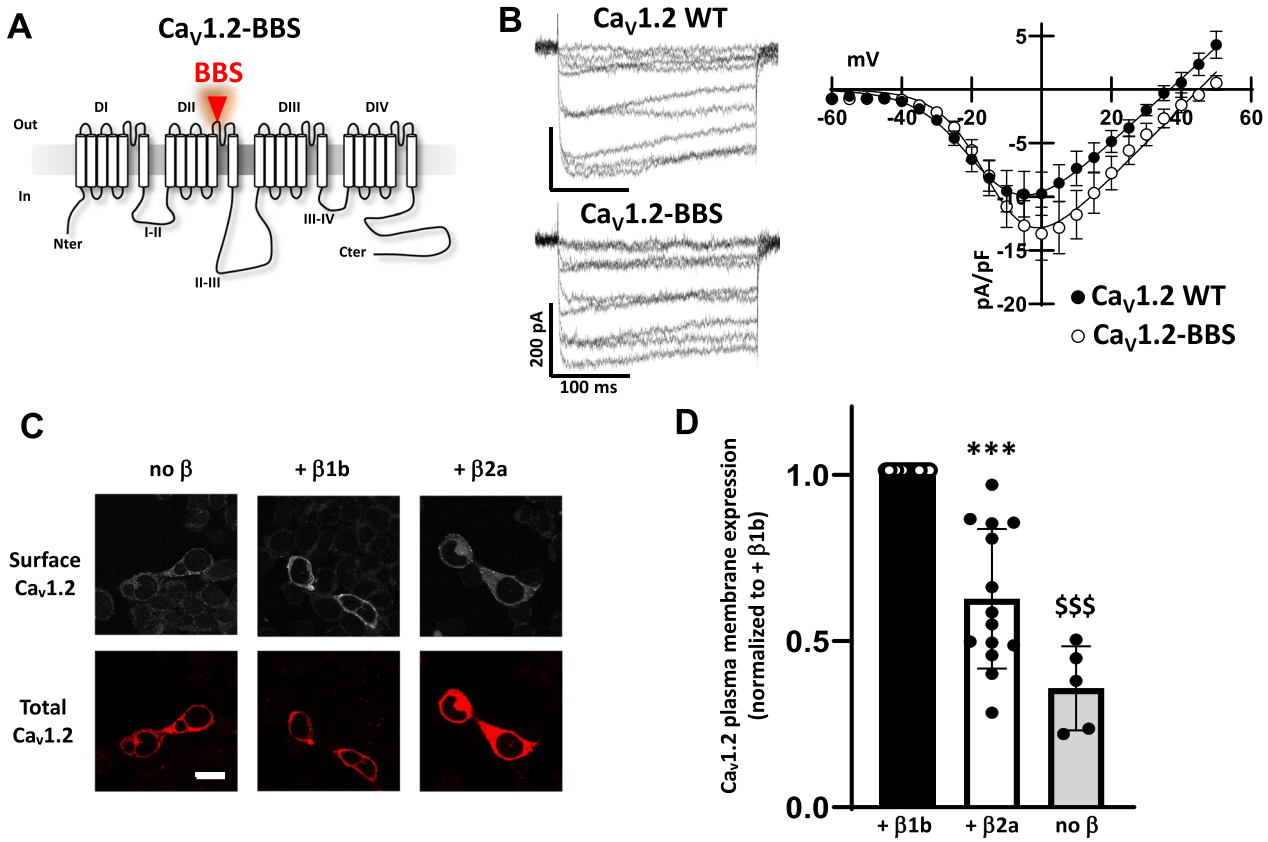

Fig. 1 Effect of Ca$_V$β subunits on Ca$_V$1.2 cell surface expression in tsA-201 cells. **a** Schematic of Ca$_V$1.2 channel tagged with bungarotoxin binding site (Ca$_V$1.2-BBS, BBS: red triangle) between S5 and the P-loop of domain II (DII). **b** Representative whole-cell current traces recorded in response to depolarizing steps from −50 to +40 mV from a holding potential of −100 mV from tsA-201 cells expressing either Ca$_V$1.2 WT (top traces) or Ca$_V$1.2-BBS (bottom traces) together with auxiliary subunits Ca$_V$α$_2$δ-1 and Ca$_V$β1b. Mean I/V curves (right panel) for Ca$_V$1.2 WT (filled circle, n = 9) and Ca$_V$1.2-BBS (open circle, n = 18) co-expressed with auxiliary subunits Ca$_V$α$_2$δ-1 and Ca$_V$β1b. **c** Confocal images showing plasma membrane expression of Ca$_V$1.2-BBS in tsA cells stained with α-bungarotoxin (BTX)-AF488 (top panels). Ca$_V$1.2-BBS was co-expressed with Ca$_V$α$_2$δ-1 (left, no β) and either Ca$_V$β1b (center) or Ca$_V$β2a (right). Cells were incubated at 17 °C with BTX-AF488 for 30 min and fixed. The cells were then permeabilized and stained with a rabbit anti-Ca$_V$1.2 Ab and secondary Ab anti-rabbit AF594 (bottom panels). Scale 20 µm. **d** Average Ca$_V$1.2-BBS surface expression co-transfected with Ca$_V$α$_2$δ-1 and either Ca$_V$β1b (black bar), or Ca$_V$β2a (open bar), or empty vector (gray bar). Bars are mean (± SEM) normalized to Ca$_V$β1b mean. ***$p < 0.001$, n = 14; $^{\$\$\$}p < 0.001$, n = 5; paired t-test, n numbers correspond to independent experiments

Results and discussion

To monitor the trafficking of Ca$_V$1.2 to the plasma membrane we introduced α-bungarotoxin binding sites in the extracellular loop of the channel (Fig. 1a). This construct, Ca$_V$1.2-BBS, remained functional and generated Ba^{2+} currents with a density similar to the WT channel (−9.7 ± 2.0 pA/pF, n = 9, vs −13.5 ± 2.5 pA/pF, n = 18, for Ca$_V$1.2-BBS and WT, respectively; Fig. 1b). However, the insertion of the tag induced a slight increase in the slope of the activation curve (from −9.3 ± 0.9 mV, n = 9, to −7.1 ± 0.3 mV, n = 18, for WT and Ca$_V$1.2-BBS, respectively, $p = 0.007$) and a depolarizing shift of the reversal potential (from 37.5 ± 2.6 mV, n = 9, to 48.4 ± 2.4 mV, n = 18, for WT and Ca$_V$1.2-BBS, respectively, $p = 0.01$). The $V_{50,act}$ and the G_{max} remained unchanged ($V_{50,act}$ = −14.5 ± 2.2 mV, n = 9, and −14.7 ± 0.6 mV, n = 18; G_{max} = 0.34 ± 0.08 nS/pF, n = 9, and 0.30 ± 0.05 nS/pF, n = 18, for WT and Ca$_V$1.2-BBS, respectively). The effect on reversal potential may be indicative of an effect of the BBS modification on permeability, but this should have little bearing on the utility of this construct for trafficking studies.

We subsequently checked the cell surface expression of Ca$_V$1.2-BBS and compared the effect of co-expressing different types of auxiliary Ca$_V$β subunits. Three days after transfection, tsA-201 cells were live-labelled with α-BTX-488 for 30 min at 17 °C, fixed and the fluorescence was quantified (Fig. 1c and d). We found that

the co-expression of $Ca_V\beta1b$ induced a 60% increase in $Ca_V1.2$-BBS surface expression compared with no $Ca_V\beta$. Additionally, although the co-expression of $Ca_V\beta2a$ also increased $Ca_V1.2$-BBS cell surface expression, its effect was not as marked as $Ca_V\beta1b$ since only a 30% increase of fluorescence was recorded (Fig. 1c and d). This result is in good agreement with a study showing differential effects of $Ca_V\beta$ subunits on $Ca_V1.2$-generated current densities, although it is important to note that interpretations of electrophysiological measurements can be confounded by effects on channel biophysics [17].

We then aimed to gain insight into the $Ca_V\beta$ subunit-dependent mechanism(s) responsible for the effects on $Ca_V1.2$ surface expression. Plasma membrane expression of $Ca_V1.2$ results from the balance between the incorporation of newly synthetized $Ca_V1.2$ from the ER, recycled $Ca_V1.2$ from endosomal compartments and the removal of channels from the plasma membrane by endocytosis [18]. We first monitored the impact of $Ca_V\beta$ subunits on $Ca_V1.2$ endocytosis by comparing the rate of internalization of $Ca_V1.2$-BBS (Fig. 2). We showed that $Ca_V1.2$-BBS, either co-expressed with $Ca_V\beta1b$ or $Ca_V\beta2a$, exhibited similar kinetics of endocytosis with a time constant of ~6 min (Fig. 2b). This is in line with previous studies on N-type calcium channels [19, 20] and measurements on cardiac cell lines [21]. We note that when $Ca_V\beta$ subunits are not co-expressed, no reduction of $Ca_V1.2$-BBS fluorescence is detected over the duration of BTX incubation

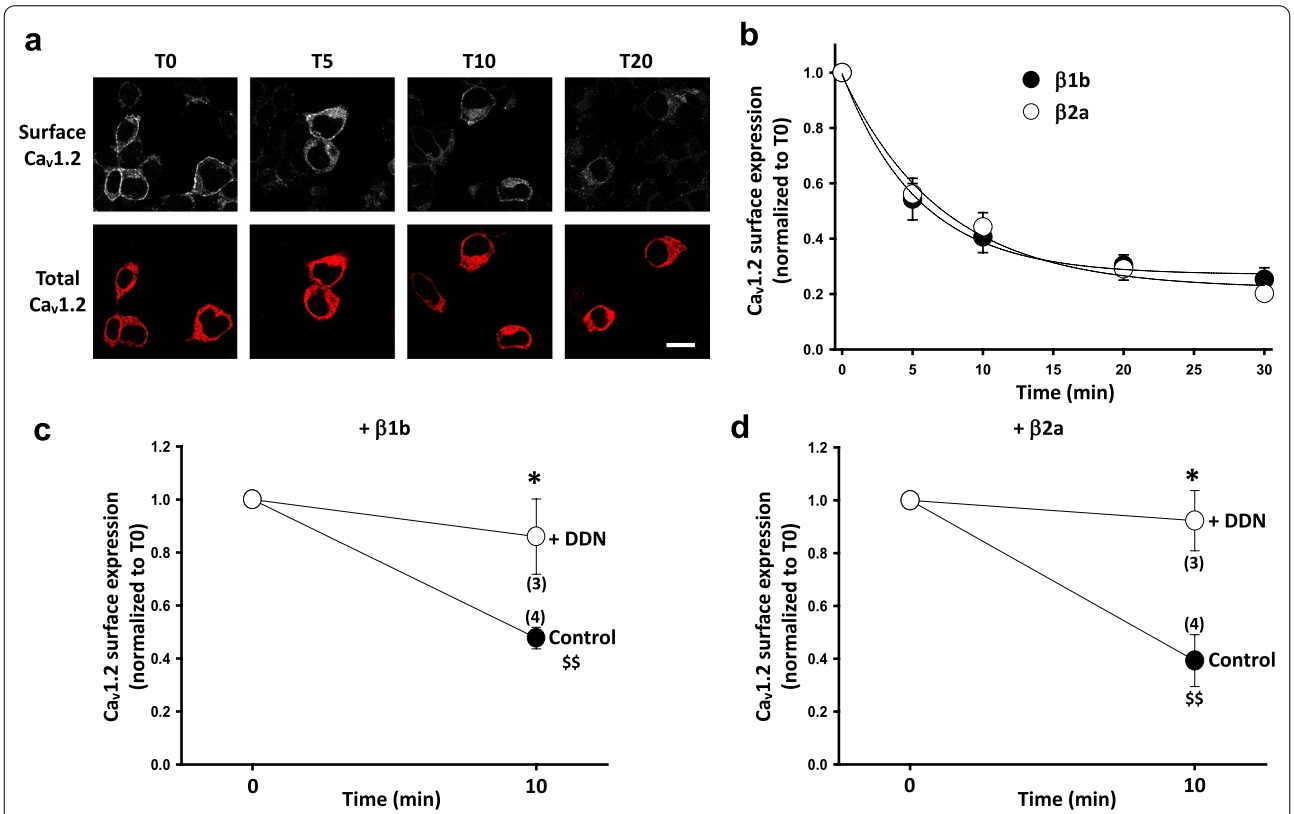

Fig. 2 $Ca_V1.2$ endocytosis is dynamin-dependent and $Ca_V\beta$ subtype-independent. **a** Representative confocal images of tsA-201 cells expressing $Ca_V1.2$-BBS and labelled with BTX-AF488 (top panels). $Ca_V1.2$-BBS was co-expressed with $Ca_V\alpha_2\delta$-1 and $Ca_V\beta1b$. Cells were incubated at 17 °C with BTX-AF488 for 30 min and then fixed at different time point after incubation at 37 °C, from zero (T0) to 20 min (T20). The cells were then permeabilized and stained with a rabbit anti-$Ca_V1.2$ Ab and a secondary Ab anti-rabbit AF594 (bottom panels). Scale bar 20 µm. **b** Time course of endocytosis of cell surface $Ca_V1.2$-BBS co-expressed with $Ca_V\alpha_2\delta$-1 and either $Ca_V\beta1b$ (filled circle) or $Ca_V\beta2a$ (open circle). The results are shown as the mean ± SEM. The n numbers correspond to independent experiments (average fluorescence from at least 25 cells per time point). The data were fitted with single exponentials. The time constants of the fits were 5.6 ± 0.2 min for $Ca_V\beta1b$ and 7.1 ± 0.2 min for $Ca_V\beta2a$, respectively. **c** and **d** Effect of dominant negative dynamin Dyn K44E on $Ca_V1.2$ endocytosis. Cells were transfected with $Ca_V1.2$-BBS, $Ca_V\alpha_2\delta$-1 and either $Ca_V\beta1b$ (**c**) or $Ca_V\beta2a$ (**d**) together with either empty pcDNA3.1 vector (filled symbols) or Dyn K44E (DDN, open symbols). Cells were incubated at 17 °C with BTX-AF488 for 30 min and then fixed at time point T0 and T20 after incubation at 37 °C. Cells were subjected to immunocytochemistry as described in **a**. BTX-AF488 fluorescence was normalized to the mean fluorescence at T0 for each condition. The results are shown as the mean ± SEM. The n numbers correspond to independent experiments (average fluorescence from at least 25 cells per time point). $^{\$\$}p < 0.01$ Control T10 vs Control T0; $^{*}p < 0.05$ DDN T10 vs Control T10, unpaired t-test

(after 20 min, $Ca_V1.2$-BBS fluorescence represented 100 ± 12% of the initial fluorescence, n = 3), suggesting that $Ca_V\beta$ subunits promote $Ca_V1.2$ endocytosis. This conclusion is different from that of a recent study showing that stabilizing the $Ca_V1.2$–$Ca_V\beta2a$ interaction via the creation of a concatemer increases the retention time of $Ca_V1.2$ at the plasma membrane in HEK-293 and HLA-1 cells [12]. However, in our experimental conditions, the starting level of $Ca_V1.2$-BBS fluorescence without $Ca_V\beta$ subunit is very low, close to the detection limit, and we cannot exclude that some endocytosis of channels may take place even in the absence of $Ca_V\beta$. It was previously shown that $Ca_V1.2$ internalization is dynamin-dependent [21]. We took advantage of the dominant negative effect of the dynamin mutant K44E [16] to show that $Ca_V1.2$ internalization depends on dynamin, regardless of co-expressed $Ca_V\beta$ subtype (Fig. 2c and d).

Next, we examined the effect of $Ca_V\beta$ subunits on net forward trafficking by monitoring the insertion of $Ca_V1.2$-BBS into the plasma membrane as a function of time (Fig. 3a and b). In the no $Ca_V\beta$ condition, $Ca_V1.2$-BBS surface expression doubled after 10 min and stayed stable during the next 40 min. However, when $Ca_V\beta$ subunits were co-expressed, we recorded an increase of $Ca_V1.2$-BBS surface expression that reached a plateau after 40 min. The increases were comparable for both $Ca_V\beta$ subunits and represented ~5 times the starting amount of $Ca_V1.2$-BBS surface expression. This is

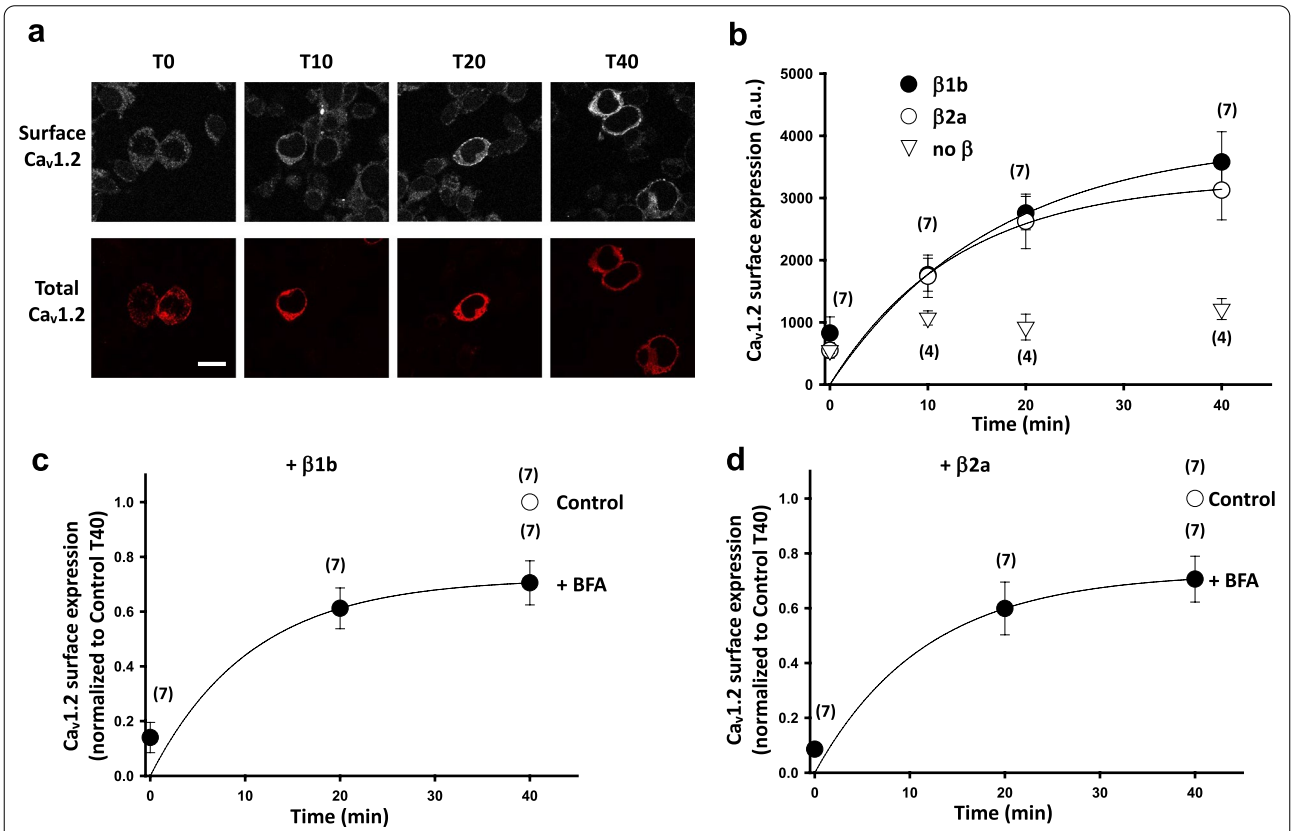

Fig. 3 $Ca_V1.2$ forward trafficking and recycling are not $Ca_V\beta$-subtype dependent. **a** Confocal images of tsA-201 cells expressing $Ca_V1.2$-BBS and labelled with BTX-AF488 (top panels). $Ca_V1.2$-BBS was co-expressed with $Ca_V\alpha_2\delta$-1 and $Ca_V\beta1b$. Cells were incubated at 17 °C with untagged BTX for 30 min and then incubated at 37 °C with BTX-AF488. The cells were fixed at different time point after incubation at 37 °C, from zero (T0) to 40 min (T40). The cells were then permeabilized and stained with a rabbit anti-$Ca_V1.2$ Ab and a secondary Ab anti-rabbit AF594 (bottom panels). Scale bar 20 µm. **b** Time course of insertion of $Ca_V1.2$-BBS at the cell surface when co-expressed with $Ca_V\alpha_2\delta$-1 and either $Ca_V\beta1b$ (filled circle), $Ca_V\beta2a$ (open circle) or empty vector (open triangle). The results are shown as the mean ± SEM (n numbers correspond to independent experiments). Data were fitted with single exponentials. The time constants of the fits were 16.8 ± 12.6 min and 13.0 ± 14.2 min for $Ca_V\beta1b$ and $Ca_V\beta2a$ (n = 7), respectively. **c** and **d** Effect of Brefeldin A (BFA) treatment on $Ca_V1.2$ forward trafficking. tsA-201 cells were co-transfected with $Ca_V1.2$-BBS, $Ca_V\alpha_2\delta$-1 and either $Ca_V\beta1b$ (**c**) or $Ca_V\beta2a$ (**d**). Cells were treated with BFA for 4 h before undergoing the forward trafficking protocol described in **a**. BTX-AF488 fluorescence was normalized to the mean fluorescence at T40 for the control condition (open circle). The results are shown as the mean ± SEM. The n numbers correspond to independent experiments (average fluorescence from at least 25 cells per time point). The data were compared using an unpaired t-test. The data were fitted with single exponentials. The time constants of the fits were 10.6 ± 6.6 min and 11.6 ± 8.1 min for $Ca_V\beta1b$ and $Ca_V\beta2a$ (n = 7), respectively

surprising, given that the steady state level of $Ca_V1.2$ is higher in the presence of the $Ca_V\beta1b$ isoform (see below).

Finally, we used BFA to disrupt the Golgi apparatus and prevent the transfer of newly synthesized channels from the ER to the plasma membrane (Fig. 3c and d). Using this strategy, we were able to estimate that 70% of the surface $Ca_V1.2$-BBS originated from a recycling pathway [21] and we could also attribute 30% to a forward trafficking process. These contributions remained identical irrespective of whether $Ca_V1.2$-BBS was co-expressed with $Ca_V\beta1b$ or $Ca_V\beta2a$ subunits. Interestingly, the contributions recycling/forward trafficking for $Ca_V2.2$ cell surface expression were reported to be closer to 50% [19, 20], although it is important to highlight the fact that these studies were performed in a neuronal cell line and that further investigations would be needed to rule out a cell-dependent effect.

Altogether, we showed that the $Ca_V\beta$ subunit subtype dependent effect on $Ca_V1.2$ surface expression was not associated with any modifications of the kinetics for forward trafficking, endocytosis and recycling. These results suggest that the level of $Ca_V1.2$ (available in the ER to be trafficked to the plasma membrane) is differentially increased in the presence of different $Ca_V\beta$ subunits. Such a mechanism is supported by the conclusions of a previous study from our group that showed that $Ca_V\beta$ subunits protect $Ca_V1.2$ from ubiquitination and degradation by the proteasome [9]. If so, then the fact that the observed effects were greater with $Ca_V\beta1b$ than with $Ca_V\beta2a$ suggests the possibility that a difference in the amount of $Ca_V1.2$ in the ER could be due to a differential ability of the two $Ca_V\beta$ subunits to protect $Ca_V1.2$ from degradation. This could potentially be due to the selective palmitoylation and membrane anchoring of $Ca_V\beta2a$ compared to the pure cytoplasmic expression of $Ca_V\beta1b$ which may have better access to the pore forming subunit in the ER. Alternatively, it is possible that the latter may be expressed at higher levels than the former and thus more effective in protecting the channel from degradation. We also consider the possibility that the protective effects of the $Ca_V\beta$ subunit may not be dependent on a physical interaction with the $Ca_V1.2$, but instead act by regulating calcium channel expression at the transcriptional or translational level. For example, for Ca_V3 calcium channels, coexpression of ancillary subunits promotes current densities despite an absence of a physical interaction [22]. On the other hand, mutation of $Ca_V1.2$ residue W440 which prevents the physical association with the $Ca_V\beta$ subunit leads to compromised membrane expression of the channel [9, 23], thus arguing against a diffuse effect on $Ca_V1.2$ protein expression. Overall, our data are consistent with a mechanism by which $Ca_V\beta$ subunits are more important for regulating the levels of $Ca_V1.2$ channels at the level of the ER, rather than directly altering the forward and reverse plasma membrane trafficking of the channel complexes. This does not negate the possibility that these subunits may be involved in modulating the targeting of $Ca_V1.2$ channels to specific sub-loci within the plasma membrane.

Acknowledgements
We thank Lina Chen for technical support.

Author contributions
LF, SG and ES collected data. LF wrote the manuscript. GWZ edited the manuscript and supervised the study. All authors read and approved the final manuscript.

Funding
This work was supported by a grant to GWZ from the Natural Sciences and Engineering Research Council of Canada. GWZ holds a Canada Research Chair.

Availability of data and materials
Data and materials will be made available based on reasonable request.

Declarations

Ethics approval and consent to participate
Not applicable.

Consent for publication
Not applicable.

Competing interests
The authors declare no competing interest.

Received: 24 March 2022 Accepted: 2 May 2022
Published online: 09 May 2022

References

1. Catterall WA, Leal K, Nanou E. Calcium channels and short-term synaptic plasticity. J Biol Chem. 2013;288:10742–9. https://doi.org/10.1074/jbc.R112.411645.
2. Wheeler DG, et al. Ca(V)1 and Ca(V)2 channels engage distinct modes of Ca(2+) signaling to control CREB-dependent gene expression. Cell. 2012;149:1112–24. https://doi.org/10.1016/j.cell.2012.03.041.
3. Catterall WA, Lenaeus MJ, Gamal El-Din TM. Structure and pharmacology of voltage-gated sodium and calcium channels. Annu Rev Pharmacol Toxicol. 2020;60:133–54. https://doi.org/10.1146/annurev-pharmtox-010818-021757.
4. Zamponi GW, Striessnig J, Koschak A, Dolphin AC. The physiology, pathology, and pharmacology of voltage-gated calcium channels and their future therapeutic potential. Pharmacol Rev. 2015;67:821–70. https://doi.org/10.1124/pr.114.009654.
5. Obermair GJ, Szabo Z, Bourinet E, Flucher BE. Differential targeting of the L-type Ca2+ channel alpha 1C (CaV1.2) to synaptic and extrasynaptic compartments in hippocampal neurons. Eur J Neurosci. 2004;19:2109–22. https://doi.org/10.1111/j.0953-816X.2004.03272.x.
6. Di Biase V, et al. Surface traffic of dendritic CaV1.2 calcium channels in hippocampal neurons. J Neurosci. 2011;31:13682–94. https://doi.org/10.1523/JNEUROSCI.2300-11.2011.
7. Buraei Z, Yang J. The ß subunit of voltage-gated Ca2+ channels. Physiol Rev. 2010;90:1461–506. https://doi.org/10.1152/physrev.00057.2009.
8. Dolphin AC. Calcium channel auxiliary α2δ and β subunits: trafficking and one step beyond. Nat Rev Neurosci. 2012;13:542–55. https://doi.org/10.1038/nrn3311.

9. Altier C, et al. The Cavβ subunit prevents RFP2-mediated ubiquitination and proteasomal degradation of L-type channels. Nat Neurosci. 2011;14:173–80. https://doi.org/10.1038/nn.2712.
10. Meissner M, et al. Moderate calcium channel dysfunction in adult mice with inducible cardiomyocyte-specific excision of the cacnb2 gene. J Biol Chem. 2011;286:15875–82. https://doi.org/10.1074/jbc.M111.227819.
11. Yang L, et al. Cardiac CaV1.2 channels require β subunits for β-adrenergic-mediated modulation but not trafficking. J Clin Invest. 2019;129:647–58. https://doi.org/10.1172/JCI123878.
12. Conrad R, Kortzak D, Guzman GA, Miranda-Laferte E, Hidalgo P. CaVβ controls the endocytic turnover of CaV1.2 L-type calcium channel. Traffic. 2021;22:180–93. https://doi.org/10.1111/tra.12788.
13. Chien AJ, Carr KM, Shirokov RE, Rios E, Hosey MM. Identification of palmitoylation sites within the L-type calcium channel beta2a subunit and effects on channel function. J Biol Chem. 1996;271:26465–8. https://doi.org/10.1074/jbc.271.43.26465.
14. Qin N, et al. Unique regulatory properties of the type 2a Ca2+ channel beta subunit caused by palmitoylation. Proc Natl Acad Sci USA. 1998;95:4690–5. https://doi.org/10.1073/pnas.95.8.4690.
15. Zhang FX, Gadotti VM, Souza IA, Chen L, Zamponi GW. BK potassium channels suppress Cavα2δ subunit function to reduce inflammatory and neuropathic pain. Cell Rep. 2018;22:1956–64. https://doi.org/10.1016/j.celrep.2018.01.073.
16. Herskovits JS, Burgess CC, Obar RA, Vallee RB. Effects of mutant rat dynamin on endocytosis. J Cell Biol. 1993;122:565–78. https://doi.org/10.1083/jcb.122.3.565.
17. Yasuda T, et al. Auxiliary subunit regulation of high-voltage activated calcium channels expressed in mammalian cells. Eur J Neurosci. 2004;20:1–13. https://doi.org/10.1111/j.1460-9568.2004.03434.x.
18. Ferron L, Koshti S, Zamponi GW. The life cycle of voltage-gated Ca^{2+} channels in neurons: an update on the trafficking of neuronal calcium channels. Neuronal Signal. 2021;5:NS20200095. https://doi.org/10.1042/NS20200095.
19. Ferron L, et al. FMRP regulates presynaptic localization of neuronal voltage gated calcium channels. Neurobiol Dis. 2020;138:104779. https://doi.org/10.1016/j.nbd.2020.104779.
20. Macabuag N, Dolphin AC. Alternative splicing in Ca(V)2.2 regulates neuronal trafficking via adaptor protein complex-1 adaptor protein motifs. J Neurosci. 2015;35:14636–52. https://doi.org/10.1523/JNEUROSCI.3034-15.2015.
21. Conrad R, et al. Rapid turnover of the cardiac L-type Ca. iScience. 2018;7:1–15. https://doi.org/10.1016/j.isci.2018.08.012.
22. Dubel SJ, et al. Plasma membrane expression of T-type calcium channel alpha(1) subunits is modulated by high voltage-activated auxiliary subunits. J Biol Chem. 2004;279:29263–9. https://doi.org/10.1074/jbc.M313450200.
23. Obermair GJ, et al. Reciprocal interactions regulate targeting of calcium channel beta subunits and membrane expression of alpha1 subunits in cultured hippocampal neurons. J Biol Chem. 2010;285:5776–91. https://doi.org/10.1074/jbc.M109.044271.

Publisher's Note